NATIONAL AND KAPODISTRIAN UNIVERSITY OF ATHENS

SCHOOL OF SCIENCES

DEPARTMENT OF INFORMATICS AND TELECOMMUNICATIONS

POSTGRADUATE PROGRAM
“DATA SCIENCE AND INFORMATION TECHNOLOGIES”

MSc THESIS

Investigation of Transition to Epileptiform Activity through the use of Phase Space Reconstruction Methodology and Complexity Metrics on Local Field Potential Signals

Kostas S. Andrikos

Supervisor: **Kostas Vekrellis,** Investigator **–** Professor Level, BRFAA

ATHENS

FEBRUARY 2024

ΕΘΝΙΚΟ ΚΑΙ ΚΑΠΟΔΙΣΤΡΙΑΚΟ ΠΑΝΕΠΙΣΤΗΜΙΟ ΑΘΗΝΩΝ

ΣΧΟΛΗ ΘΕΤΙΚΩΝ ΕΠΙΣΤΗΜΩΝ
ΤΜΗΜΑ ΠΛΗΡΟΦΟΡΙΚΗΣ ΚΑΙ ΤΗΛΕΠΙΚΟΙΝΩΝΙΩΝ

ΠΡΟΓΡΑΜΜΑ ΜΕΤΑΠΤΥΧΙΑΚΩΝ ΣΠΟΥΔΩΝ
"ΕΠΙΣΤΗΜΗ ΔΕΔΟΜΕΝΩΝ ΚΑΙ ΤΕΧΝΟΛΟΓΙΕΣ ΠΛΗΡΟΦΟΡΙΑΣ"

ΔΙΠΛΩΜΑΤΙΚΗ ΕΡΓΑΣΙΑ

Διερεύνηση της Μετάβασης σε Επιληπτικόμορφη Δραστηριότητα μέσω της χρήσης της μεθοδολογίας Ανακατασκευής του Χώρου των Φάσεων και Μετρικών Πολυπλοκότητας σε Σήματα Δυναμικού Τοπικού Πεδίου

Κώστας Σ. Ανδρίκος

Επιβλέπων: **Κώστας Βεκρέλλης, Διευθυντής Ερευνών ΙΙΒΕΑΑ**

ΑΘΗΝΑ

ΦΕΒΡΟΥΑΡΙΟΣ 2024

MSc THESIS

Investigation of Transition to Epileptiform Activity through the use of Phase Space Reconstruction Methodology and Complexity Metrics on Local Field Potential Signals

Kostas S. Andrikos
DS2190002

SUPERVISOR: **Kostas Vekrellis**, Investigator – Professor Level, BRFAA

EXAMINATION COMMITTEE:

Irini Skaliora, Professor of Cognitive Science
Director of MSc Program in Cognitive Science
Department of the History and Philosophy of Science
University of Athens

Affiliated Investigator
Neurophysiology Laboratory
Center for Basic Research
BRFAA

Elias Manolakos, Professor, Department of Informatics and Telecommunications
University of Athens

February 2024

ΔΙΠΛΩΜΑΤΙΚΗ ΕΡΓΑΣΙΑ

Διερεύνηση της Μετάβασης σε Επιληπτικόμορφη Δραστηριότητα μέσω της χρήσης της μεθοδολογίας Ανακατασκευής του Χώρου των Φάσεων και Μετρικών Πολυπλοκότητας σε Σήματα Δυναμικού Τοπικού Πεδίου

Κώστας Σ. Ανδρίκος
Α.Μ.: DS2.19.0002

ΕΠΙΒΛΕΠΩΝ: **Κώστας Βεκρέλλης**, Διευθυντής Ερευνών, ΙΙΒΕΑΑ

ΕΞΕΤΑΣΤΙΚΗ ΕΠΙΤΡΟΠΗ:

Ειρήνη Σκαλιώρα, Καθηγήτρια Γνωσιακής Επιστήμης
Δ/ντρια Μεταπτυχιακού Π.Σ. στην Γνωσιακή Επιστήμη
Τμήμα Ιστορίας και Φιλοσοφίας της Επιστήμης
Εθνικό και Καποδιστριακό Πανεπιστήμιο Αθηνών

Συνεργαζόμενη Ερευνήτρια
Εργαστήριο Νευροφυσιολογίας
Κέντρο Βασικής Έρευνας
ΙΙΒΕΑΑ

Ηλίας Μανωλάκος, Καθηγητής, Τμήμα Πληροφορικής και Τηλεπικοινωνιών
Εθνικό και Καποδιστριακό Πανεπιστήμιο Αθηνών

Φεβρουάριος 2024

ABSTRACT

As epilepsy, the most common neurological disorder, affects millions of people, any work elucidating aspects of the mechanisms underlying this disorder may be of valuable importance. We have used the Phase Space Reconstruction methodology to gain insights on the transition from the spontaneous Up/Down states network activity of ex vivo cortical slices, considered the default cortex activity, to a steady state hypersynchronous epileptiform state. This is a complex phenomenon, not following strict stereotypical paths of evolution.

Our results show that the system dynamics shift long before the stable epileptic state is observed. This is especially surprising in the case of the quiescent signal segments analysis. This shift is characterized by a loss of complexity and an increase in the signal's regularity. This result may be used as a means for predicting the occurrence of the epileptiform state, on one hand, and as confirmation of studies relating complexity to normal brain activity, on the other.

SUBJECT AREA: Signal Processing, Computational Neuroscience, Electrophysiology

KEYWORDS: local field potential, phase space reconstruction, epilepsy, nonlinear metrics, complexity

ΠΕΡΙΛΗΨΗ

Καθώς η επιληψία, η συχνότερη νευρολογική διαταραχή, επηρεάζει εκατομμύρια ανθρώπους, κάθε εργασία που διερευνά πτυχές των μηχανισμών που βρίσκονται πίσω από αυτήν την διαταραχή, μπορεί να προσφέρει πολύτιμη βοήθεια. Χρησιμοποιήσαμε τη μεθοδολογία Ανακατασκευής του Χώρου των Φάσεων για να οδηγηθούμε σε μία βαθύτερη κατανόηση σχετικά με τη μετάβαση από την αυθόρμητη δικτυακή δραστηριότητα της δισταθούς κατάστασης UP/Down σε τομές φλοιού ex vivo, η οποία θεωρείται η προκαθορισμένη/τυπική δραστηριότητα του φλοιού, σε μια σταθερή υπερσύγχρονη επιληπτικόμορφη κατάσταση. Πρόκειται για ένα πολύπλοκο φαινόμενο, που δεν ακολουθεί αυστηρά στερεότυπες διαδρομές εξέλιξης.

Τα αποτελέσματά μας δείχνουν ότι οι δυναμικές του συστήματος μεταβάλλονται πολύ πριν παρατηρηθεί η σταθερή επιληπτικόμορφη κατάσταση. Αυτό είναι ιδιαίτερα απρόσμενο όσον αφορά στα τμήματα του σήματος χωρίς δραστηριότητα. Η μεταβολή αυτή χαρακτηρίζεται από μείωση της πολυπλοκότητας και αύξηση της κανονικότητας του συστήματος. Το αποτέλεσμα αυτό μπορεί να χρησιμοποιηθεί ως μέσο πρόβλεψης της επιληπτικόμορφης κατάστασης, αφενός, και ως επιβεβαίωση μελετών που συσχετίζουν την πολυπλοκότητα με τη φυσιολογική δραστηριότητα του εγκεφάλου, αφετέρου.

ΘΕΜΑΤΙΚΗ ΠΕΡΙΟΧΗ: Επεξεργασία Σήματος, Υπολογιστική Νευροεπιστήμη, Ηλεκτροφυσιολογία

ΛΕΞΕΙΣ ΚΛΕΙΔΙΑ: δυναμικό τοπικού πεδίου, ανακατασκευή του χώρου των φάσεων, επιληψία, μη-γραμμικές μετρικές, πολυπλοκότητα

ACKNOWLEDGEMENTS

First and foremost, I am immensely grateful to PhD candidate Michael Vinos for without his unwavering scientific and moral support this endeavor would not have been possible. I would also like to thank Professor Irini Skaliora for her patience and invaluable feedback. Special thanks to Nikos Vassilopoulos MSc for his expertise.

I would like to express my appreciation to the faculty of the Biomedical Research Foundation of the Academy of Athens (BRFAA), the Department of Informatics and Telecommunications of the University of Athens and the ATHENA Research Center as their efforts, guidance and high academic expertise have been crucial in shaping my educational journey throughout the entire program.

Lastly, I cannot express enough gratitude to my family, especially my wife and children for their encouragement and tolerance.

CONTENTS

LIST OF FIGURES

LIST OF TABLES

1. INTRODUCTION

1.1 Epilepsy and Electrophysiology

Epilepsy is a chronic brain disorder, characterized by recurring abnormal electrical disturbances called seizures. Seizures can cause a variety of changes in behavior, movements or consciousness, from brief lapses of attention, to severe shaking. Epilepsy affects around 50 million people of all ages worldwide, making it the most common neurological disorder according to the World Health Organization [1].

Several electrophysiology techniques, such as Electroencephalogram (EEG) and Magnetoencephalography (MEG) are used to produce brain signals useful for studying epilepsy. Local Field Potentials (LFP) is one of them. These potentials are usually captured by the use of a single recording micro-electrode, or an array of micro-electrodes placed in the extracellular space of the brain tissue. The extracellular currents produced by synaptic activities in dendrites of pyramidal neurons are those that give rise to the LFP. An electrode samples the average activity within an area which is typically in the range of hundreds of micrometers to a few millimeters around it. In contrast to the EEG method which covers a large population of neurons, LFPs are sampled from a localized population of neurons [2]. Thus, LFPs can give insight into the local processes and dynamics of the network, capturing an intermediate scale between the single neuron recording and wide range recordings like the EEG [3].

The method is used both in vivo, for example during a brain surgery, and in vitro as in the case of the present study, mostly on rodent brain slices. This method is also referred to as an “ex vivo” method. Mice brain tissues are sliced and preserved in suitable chemical solution, keeping their spontaneous activity for hours. The method gives comparably good results, and thus is considered to be a useful alternative to the in vivo one [4].

LFPs have been used in several of studies concerning epilepsy aspects [5], [6].

1.2 The PSR method

A dynamical system is a system that evolves through time and is described by a set of variables. At each time point, the values of this set of variables define the “state” of the system. Thus, geometrically, we can represent the state of a dynamical system as a point in a multi-dimensional space, the State or Phase Space. The system evolves through time passing from one state to the next following a rule, which can be described by a set of differential equations. If this rule is a nonlinear function of the state, the system is called a nonlinear dynamical system [7]. By depicting each state of the system in the Phase Space we create a trajectory that completely describes the evolution of the system through time. In Figure 1 [8] we can see examples of one-dimensional time-series on the left and their respective reconstructed phase space on the right.

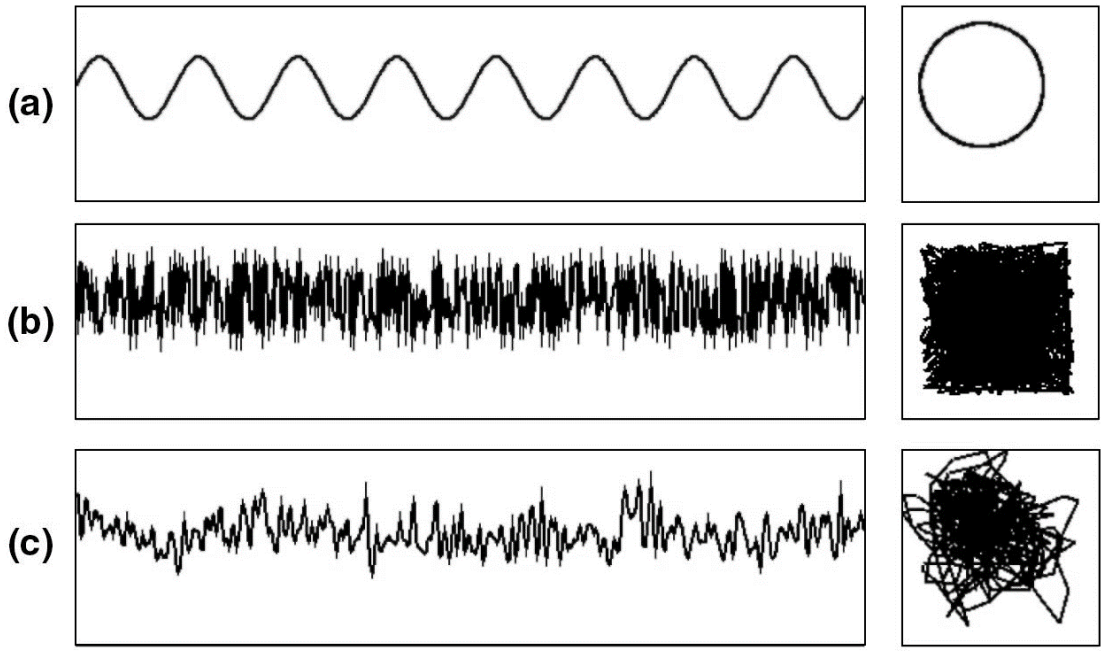

Figure 1: Phase space reconstruction patterns: (a) harmonic oscillator, (b) random oscillator, (c) EEG data (adapted from Dawid, 2019 [8])

One of the most powerful tools used in the study of nonlinear dynamical systems is the Phase Space Reconstruction method. Takens' Embedding Theorem [9] and the work of other researchers like Packard [10], provide the mathematical foundation supporting the PSR method. The power of the PSR method lies in the fact that using a one-dimensional time series coming from our multivariable system, we can create a Reconstructed Phase Space that, although different from the original one, preserves the dynamics of the system.

An example of Phase Space Reconstruction is the Roessler System. The system has three variables, namely x,y,z, and is described by the following system of differential equations:

$$\frac{dx}{dt} = -y - z$$

$$\frac{dy}{dt} = x + ay$$

$$\frac{dz}{dt} = b + z(x - c)$$

Solving the system for a=0.1, b=0.1, c=10.0 and initial conditions x(0)=5, y(0)=5, z(0)=1, we get the functions x(t), y(t), z(t) depicted in Figure 2 [11].

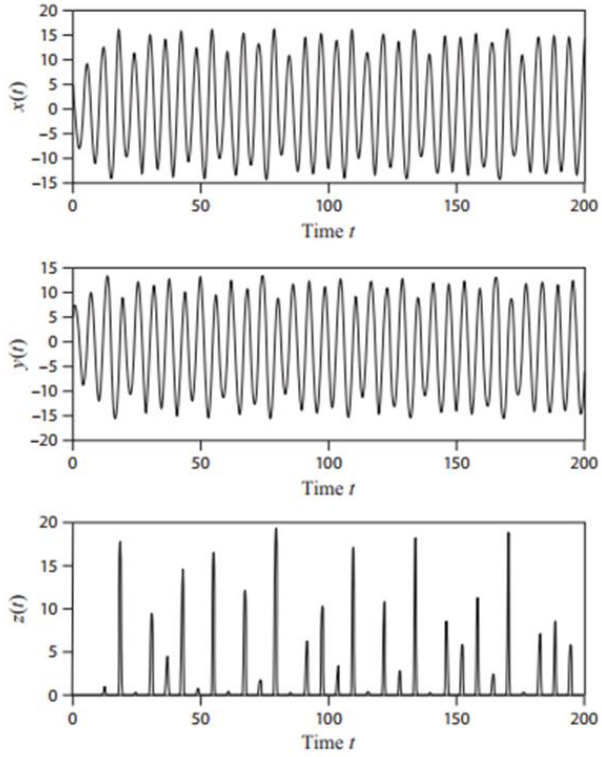

Figure 2: A solution of the Roessler System (Feldman, 2019 [11])

By representing the states of the system, that is the triplets [$x(t_i)$, $y(t_i)$, $z(t_i)$] for every time point t_i of the solution above, in a three-dimensional space, we get the Phase Space of the particular solution shown in Figure 3 [11], which fully describes the behavior of the system. The bold dot represents the initial conditions triplet.

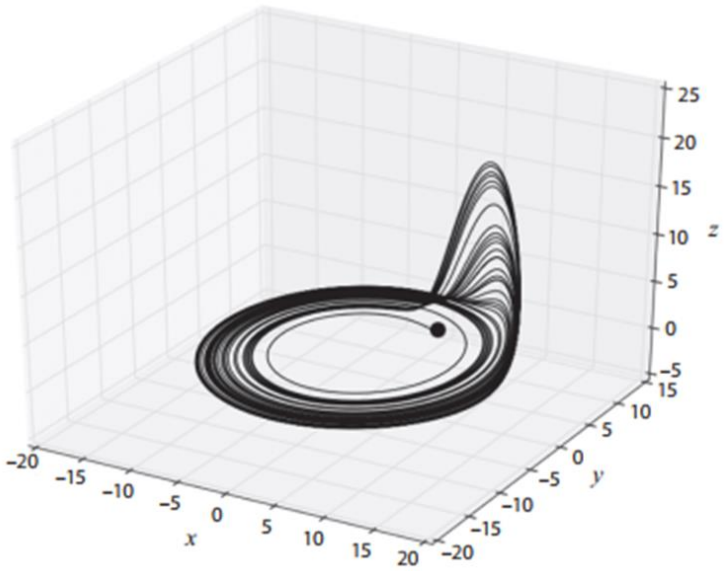

Figure 3: The Phase Space of a Roessler System Solution (Feldman, 2019 [11])

Let's now assume that only one of the three solution functions is known to us through observation/measurement, namely x(t). For each time point $x(t_i)$ of x(t) we create a triplet [$x(t_i)$, $x(t_i - \tau)$, $x(t_i - 2\tau)$], where $x(t-\tau)$ and $x(t-2\tau)$ are τ and 2τ delayed versions of x(t) respectively. This procedure is called Embedding and creates a new triplet of functions,

$[x(t_i), x(t_i - \tau), x(t_i - 2\tau)]$, in the place of the original one [x(t), y(t),z(t)]. Embedding requires an appropriate choice of the embedding dimension (m), here m=3, and the time delay (τ). In practice, τ is chosen first and then m is determined. Several algorithms lead to the choice of these parameters [12]. If we now create the phase space of these three "new" variables we get the Reconstructed Phase Space shown in Figure 4 [11] which preserves the dynamics of the original system [9],[10].

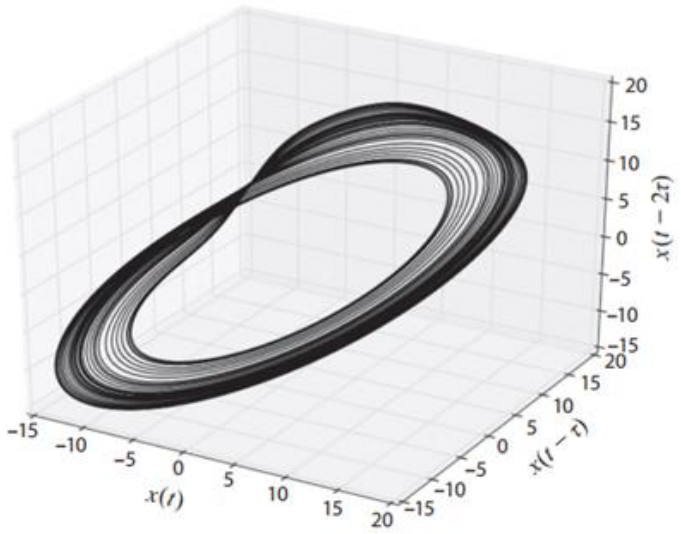

Figure 4: Reconstructed Phase Space of the Roessler System, (Feldman, 2019 [11])

By applying suitable metrics on this reconstructed phase space we can gain valuable insights regarding the system's complexity, predictability, regularity or stability [12].

Thus, through the use of a one-dimensional time series the PSR method provides us the means to understand, characterize or even predict the behavior of a complex dynamical system [12]. The power and effectiveness of the method has made it a frequently used tool in a diversity of scientific fields covering engineering, economics, neuroscience and biology among others.

1.3 Present study

Several epilepsy researchers, for example Lee [13], Sharma & Pachori [14], and Dawid [8] have used EEG signals and the PSR method to extract features aiming to develop classifiers that can effectively classify a given signal segment as normal, pre-ictal, or ictal. Pre-ictal is considered to be the state of an epileptic brain before the epilepsy events occur. Ictal is the state of an epileptic brain when epileptic seizures become its dominant activity.

In the present study we try to gain insights into epilepsy dynamics, and more specifically, on the transition from spontaneous brain activity to the epileptic one. The aim is not to classify signal segments but to develop perspectives into the process of ictogenesis, investigating the transition of the system from the spontaneous physiological activity to the epileptic state. LFP signals from mouse brain slices are used as data. Our signals start with the Control (spontaneous, non-epileptic activity), and include the entire phenomenon evolution up to the emergence of epileptic events. We try to investigate the phenomenon in its continuous and uninterrupted development. A significant difference from previous studies is that our PSR assisted investigation of the transition to epilepsy

starts from the default-spontaneous Up/Down state which is captured in the Control signal segments.

The PSR method, suitable for nonlinear signals as in case of the LFPs, is applied to create reconstructed phase spaces. In Figure 5, the (one-dimensional) LFP of the spontaneous-normal activity signal of an specific experiment and the corresponding reconstructed three-dimensional phase space are shown.

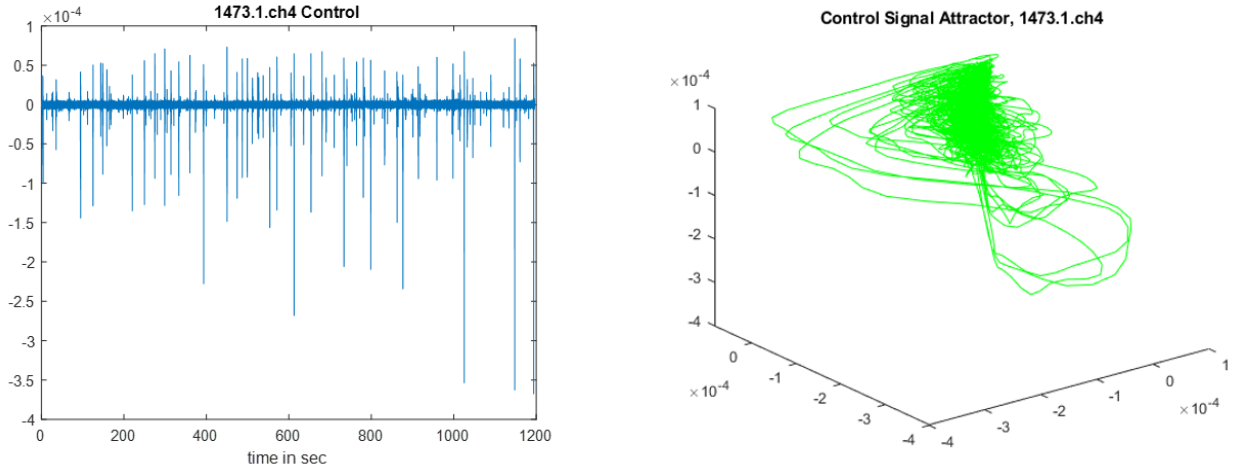

Figure 5: One-dimensional LFP signal (left) and its PSR reconstruction (right)

By applying metrics such as the Lyapunov Exponents, the Correlation Dimension and several Entropies on the Reconstructed Phase Space, we may infer conclusions about the regularity, the complexity, the stability, the randomness or the degree of chaotic behavior of the system and thus gain insights about the underlying system dynamics. All metrics chosen are met frequently in literature for the analysis of non-linear and non-stationary signals as the LFPs we use here. The Lyapunov exponent is used to measure the sensitivity of a system to initial conditions, a crucial indication of how chaotic or not a system is. Correlation Dimension helps us evaluate the dimensional complexity of the system. Entropies measure the predictability, complexity, regularity or randomness and the stability of a system.

The PSR method was applied to three parts of the dataset:

1. The entire LFP signal recorded. This is considered to be a continuous signal starting from the “normal”-spontaneous activity phase and ending to the epileptic (ictal) phase.

2. The quiescent parts of the signal. These are the baseline, parts of the signal that occur between events and are characterized by minimal neuronal activity

3.The active parts of the signal that include events. That refers to upstates (during the period of endogenous normal activity), or inter-ictal or SLE events that occur following the switch to 0 Mg condition and leading to the stable epileptiform activity.

The goal of this thesis is to investigate whether there are significant changes in the system’s dynamics on its transition from the default-spontaneous Up/Down states network activity to the epileptiform activity.

In section 2, “MATERIALS and METHODS” the details regarding the data used, and the methodologies applied on them are presented. Section 3, “RESULTS and DISCUSSION” presents our findings and discusses their significance regarding brain dynamics. Section 4 “CONCLUSION and FURTHER RESEARCH”, summarizes our findings, and proposes ideas to extent the present work.

2. MATERIALS and METHODS

2.1 Animals

C57Bl/6J mice were bred in the animal facility of the Center for Experimental Surgery of the Biomedical Research Foundation of the Academy of Athens. The facility is registered as a breeding and experimental facility according to the Presidential Decree of the Greek Democracy 160/91, which harmonizes the Greek national legislation with the European Council Directive 86/609/EEC on the protection of animals used for experimental and other scientific purposes. The present study was approved by the Regional Veterinary Service, in accordance to the National legal framework for the protection of animals used for scientific purposes (reference number 2834/08-05-2013). Mice were weaned at 21 days old (do), housed in groups of 5–10, in 267 × 483 × 203 mm cages supplied with bedding material and kept at a 12–12 dark-light schedule. Food was provided ad libitum [4].

2.2 Slice Preparation

Coronal brain slices (400 μm) were prepared from the primary somatosensory cortex of the whiskers [i.e., barrel cortex, S1BF; anterior–posterior from Bregma (A/P): −.82 to −1.94 mm, MedialLateral (M/L): 2.50 to 4.00 mm]. Young mice (P18-P20, male and female) were sacrificed with cervical dislocation, and the brain was rapidly extracted and placed in oxygenated (95% O2–5% CO2) ice-cold dissection buffer containing, in mM: KCl 2.14; NaH2PO4. H2O 1.47; NaHCO3 27; MgSO4 2.2; D-Glucose 10; Sucrose 200; and CaCl2.2H2O 2; osmolarity (mean ± SD): 298 ± 5 mOsm, pH: 7.4 ± .2. Brain slices were cut using a vibratome (VT 1000 S, Leica) and placed in a holding chamber with artificial cerebrospinal fluid (ACSF) containing (in mM): NaCl 126; KCl 3.53; NaH2PO4.H2O 1.25; NaHCO3 26; MgSO4 1; D-glucose 10 and CaCl2.2H2O 2 [osmolarity (mean ± SD): 317 ± 4 mOsm, pH: 7.4 ± .2], where they were left to recover at room temperature (RT: 24–26°C) for at least 1 h prior to recording [15].

2.3 Ex vivo electrophysiology

Following a 1-h recovery, slices were transferred to a modified submerged type of chamber (Luigs & Neumann, Ratingen Germany) coated with a layer of transparent silicone onto which up to four slices could be pinned, to maximize yield and compare different experimental groups under identical conditions. The slices were perfused at high flow rates (10–15 ml/min) by means of a vacuum pump to ensure optimal oxygenation of the cortical tissue [16]. Recordings of endogenous cortical activity were performed in “in vivo-like” ACSF (composition same as above, but with 1 mM CaCl2) at room temperature (RT: 24–27°C), after 1 h of incubation in the submerged chamber [17], [18], [4], [19]. After recording spontaneous cortical activity for 20 min, temperature was raised to 32–35°C and epileptiform activity was induced with the low Mg2+, in which the “in vivo-like” ACSF either lacked Mg2+ ions. The slices were perfused for up to 80 min to ensure that the pattern of epileptiform activity had stabilized. Network activity was assessed by local field potential (LFP) recordings which were obtained from cortical layers II/III of S1BF using

low impedance (~.5 MΩ) glass pipettes filled with ACSF. Pipettes were made from borosilicate glass (1.5 mm o.d, .86 mm i.d, with inner filament) and pulled using a P-97 micropipette puller (Sutter Instrument Co., Novato, CA, USA). Recordings were obtained in current-clamp mode with a Multiclamp 700B amplifier (Molecular Devices, San Jose, CA, USA). LFP signals were low-pass filtered at 6 kHz (by an analog anti-aliasing filter) and subsequently digitized at 15 kHz by means of a 16-bit multi-channel interface (InstruTECH ITC-18; HEKA Elektronic, Lambrecht, Germany). Data acquisition was accomplished using AxoGraph X (version 1.3.5; https://axogr aph.com; RRID:SCR_014284). The above protocols were used by Vasilopoulos et al. [15] to produce the LFP signals used in this study.

2.4 Data analysis

The LFP signals (0-200 Hz range of the raw signal) from six (6) of the experiments described above were analyzed. Each experiment consists of five (5) LFP segments of the activity from acute cortical slices of mouse brain. Each recording has a duration of 20 min, a sampling rate of 15385 Hz, and is downsampled by a factor of five (5) down to 3077 Hz.

The first of these five recordings is the Control signal, which depicts the spontaneous (normal) brain activity in the form of Up and Down states. After this first Control recording, epileptiform activity is induced with the low Mg2+ and four more 20 min recordings are analyzed. Usually, the slice becomes epileptic during the second or the third of these recordings.

This whole 5x20 min signal is divided into three periods of interest, namely the Control as stated above, the Pre-Ictal, and the Ictal (or SLA, seizure-like activity) segments.

The Control period is considered to be the one of spontaneous (non-epileptic) activity. The Pre-Ictal is the period that starts with the application of the low Mg2+ condition and ends when the seizure-like activity begins. It can be further divided into Pre-SD and Post-SD segments where SD is the Spreading Depolarization wave. Finally, the Ictal period is the one with the seizure-like activity. In the following figure (Figure 6) the whole 5x20 min recording of one of the experiments studied is presented.

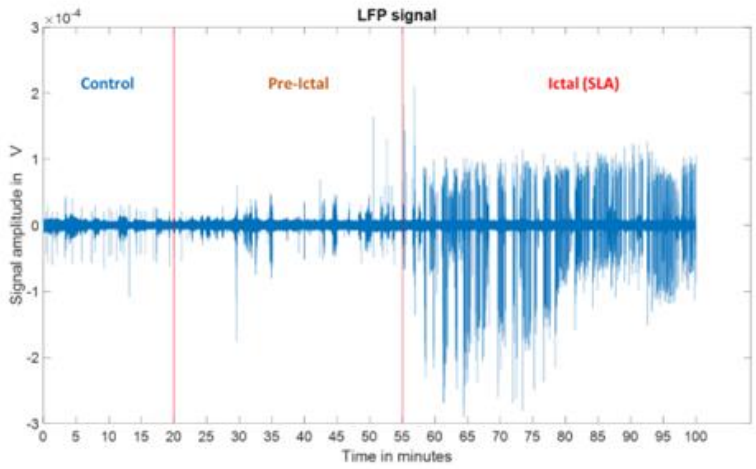

Figure 6: Whole LFP signal as recorded in one of the experiments

All signal periods from all six experiments are sliced to 1 sec, 2 sec or 5 sec non-overlapping segments. To each segment the Phase Space Reconstruction method is applied with dimension dim=3 and time lag tau=13 data points.

The value of dim=3 was chosen for several reasons. Firstly, an optical representation of the system's attractors is made possible. Secondly, the calculation of various metrics is also optimized for a low value of dimension such as dim=3. Lastly, values of between 3 and 7 are the most commonly used in literature [8].

The value of tau=13 was the most frequent one found with the average mutual information minima method, among all segments.

After applying the PSR method, the data is transformed to the reconstructed phase space, that is, a series of three component (dim=3) vectors. To these vectors created, several nonlinear metrics, most of which are derived from the dynamical systems theory, are applied. More specifically the Lyapunov Exponent, Correlation Dimension and several Entropies were used.

For each of the six experiments, and for each metric, the mean value of the metric was calculated for each of the three (Control, Pre-Ictal, Ictal) or four (Control, Pre-SD, Post-SD, Ictal) periods of interest. These six mean values for each period are statistically compared with repeated-ANOVA test with the six mean values of the other two (or three) periods as shown in the table that follows.

Table 1:Representation of the data groups compared with R-ANOVA

	Metric A		
	Control	Pre-Ictal	Ictal
Experiment1	mean_C1	mean_P1	mean_Ic1
Experiment2	mean_C2	mean_P2	mean_Ic2
Experiment3	mean_C3	mean_P3	mean_Ic3
Experiment4	mean_C4	mean_P4	mean_Ic4
Experiment5	mean_C5	mean_P5	mean_Ic5
Experiment6	mean_C6	mean_P6	mean_Ic6

The three groups compared with R-ANOVA are the Control (mean_Cx) group, the Pre-Ictal (mean_Px) group and the Ictal (mean_Icx) group.

We first applied the phase-space reconstruction analysis to the entire signal (including both quiescent segments and events) for the three periods of interest:

(a) control = endogenous activity in the form of Up and Down states,

(b) pre-ictal = period between the switch to the 0Mg solution and the first mature ictal events (as identified by expert users); and

(c) ictal = period from the first SLE to the end of the recording.

The same method is applied, considering only quiescent signal segments with the addition of 1 sec non-overlapping windows and active signal segments from each experiment and period of interest.

The aim is to test if any of the metrics have statistically significant differences between the signal periods of interest and if so to justify a biological explanation over them.

All calculations were done in Matlab, using Matlab's functions and the EntropyHub toolkit [20].

2.5 Comments on certain metrics

Before presenting the analysis results, some comments on the metrics that appear to be of interest, are due.

Conditional entropy (CondEn): Conditional entropy and its variants are used as a measure of predictability and regularity in a time series, as they provide a means to quantify how much the knowledge of past values can help us predict the future ones. A decrease in *Conditional Entropy* as we move from one part of the signal to the next suggests the system becomes more predictable and regular. Porta et. al [21], applied conditional entropy to measure regularity in sympathetic outflow time series.

Cosine Similarity Entropy (CoSiEn): The CoSiEn is a metric that assesses the structural complexity of time series using the angular distance to calculate the similarity between embedding vectors. CoSiEn has been demonstrated to quantify degrees of self-correlation-based complexity in a time series rather than to quantify degrees of uncertainty-based complexity as in the case of Sample Entropy and Fuzzy Entropy [22]. This means that a high CoSiEn value indicates a signal with increased self-correlated complexity. Increased self-correlated complexity can be related to the emergence of patterns and a transition to a more predictable state. Self-correlated complexity can be linked with self-correlation or autocorrelation of a signal, but is a broader concept involving attributes of a systems internal structure.

Spectral Entropy (SpecEn): Spectral Entropy is different compared to all other metrics used, in the sense that it is not applied to the reconstructed phase space but to the time series itself and more specifically to the Power Spectral Density (PSD) of the time series. It has been used in many EEG related studies. For example, Helakari et. al [23] use Spectral Entropy as a measure of spectral signal irregularity to study epileptiform activity. Inouye et al. [24], were the first to use Spectral Entropy for the quantification of EEG irregularity. A high Spectral Entropy value indicates a signal with approximately uniform distribution of power over the various frequencies. This means that the signal is more complex or less predictable. On the other hand, a lower Spectral Entropy suggest a more predictable and less complex signal, as only certain frequencies dominate.

Bubble Entropy (BubblEn): As other entropies, Bubble Entropy [25] is used to measure the regularity and the complexity of a dynamical system. A high Bubble Entropy value indicates a signal that is unpredictable and complex. On the other hand, a decrease in Bubble Entropy signals a transition of the system to a more ordered, predictable state.

Renyi Entropy (RenyiEn): Renyi Entropy is a generalization of the widely known and used Shannon entropy. A smaller Renyi Entropy means that a time series is less complex and more predictable. Variants of Renyi Entropy have been used for classification of epileptic EEG signals [26], [27].

All entropies used in the analysis of dynamical systems measure the complexity, randomness, regularity or predictability of the system. Yet doing so, each utilize different approaches, algorithms and concepts. For example, Spectral Entropy uses the frequency domain of a signal, whereas Bubble Entropy focus on specific segments of the signal, the "bubbles" and estimates the predictability by searching for patterns in these bubbles.

Lyapunov Exponent (LyapExp): The largest Lyapunov Exponent is a measure of the convergence/divergence of nearby trajectories in a system's phase space. The larger the exponent the faster two close-by trajectories diverge, meaning that the system is sensitive to initial conditions thus more chaotic and less predictable. The Lyapunov exponent has been used to study brain signals and epilepsy in particular by Iasemidis et al. [28].

3. RESULTS and DISCUSSION

3.1 Results using the entire signal divided in three (3) time periods

We first applied the phase-space reconstruction analysis to the entire signal (including both quiescent segments and events) for the three periods of interest:

(a) control = endogenous activity in the form of Up and Down states,

(b) pre-ictal = period between the switch to the 0Mg solution and the first mature ictal events (as identified by expert users); and

(c) ictal = period from the first SLE to the end of the recording.

The results of the entire signal analysis for 2 sec and 5 sec non-overlapping windows, are shown in Table 2.

Table 2: RANOVA results for the entire signal, 2 sec windows (left), 5 sec windows (right), 3 time periods

RANOVA (Entire signal 2sec windows, 3 periods)	Control-Pre ictal	Control-Ictal	Pre ictal-Ictal
Metric			
Lyapunov Exponent		↘	↘
Correlation Dimension		~↘	↘
Approximate Entropy		↘	↘
Sample Entropy		↘	↘
Fuzzy Entropy			
Kolmogorov Entropy		↘	↘
Permutation Entropy			
Conditional Entropy	↘	↘	↘
Distribution Entropy		~↘	
Spectral Entropy	↘	↘	
Dispersion Entropy		↘	↘
Increment Entropy			
Cosine Similarity Entropy	↗	↗	
Phase Entropy			
Bubble Entropy			
Renyi Entropy			
Entropy of Entropy		↘	↘
Average Shannon Entropy		↘	↘

RANOVA (Entire signal 5sec windows, 3 periods)	Control-Pre ictal	Control-Ictal	Pre ictal-Ictal
Metric			
Lyapunov Exponent		↘	↘
Correlation Dimension		~↘	↘
Approximate Entropy		↘	↘
Sample Entropy		↘	↘
Fuzzy Entropy			
Kolmogorov Entropy		↘	↘
Permutation Entropy			
Conditional Entropy		↘	↘
Distribution Entropy		↘	
Spectral Entropy	↘		
Dispersion Entropy		↘	↘
Increment Entropy			
Cosine Similarity Entropy	↗	↗	
Phase Entropy			
Bubble Entropy			
Renyi Entropy			
Entropy of Entropy		↘	↘
Average Shannon Entropy		↘	↘

The arrows indicate that there is a statistically significant difference between the two periods mentioned on top of the column. Statistically significant differences are considered those that resulted a p-value less than 0.05 in the R-ANOVA test. The direction of the arrows shows a relative increase (up) or decrease (down). For example, an arrow directed downwards in the column “Control-Pre Ictal” for a specific metric indicates a statistically significant decrease for the metric in the Pre Ictal period, compared to the Control one. Arrows in gray boxes with the tilt (~) are cases close to statistical significance, that is with a p-value less than 0.10.

As the system enters a stable epileptic state (Ictal period) it becomes more regular and predictive due to the repetition of seizure-like events. Hence, we would expect to find that many entropy metrics decrease in the ictal period, compared to either the Control and the pre-Ictal period. This was indeed the case for the Lyapunov exponent, Correlation Dimension and many of the Entropy metrics.

The results appear to be quite similar for the cases of the 2 sec and 5 sec windows, indicating that most of the dominant patterns are captured inside the 2 sec window.

Less expected were the changes in three Entropy metrics, *Conditional*, *Spectral* and *Cosine Similarity Entropies* for the case of the 2 sec windows, which also showed significant differences between the Control and the Pre-Ictal periods. This is an indication that after the 0 Mg condition is applied, we have a shift in the system's dynamics. The system transits into a new state, different from the normal one captured by the Control signal, although it does not yet exhibit clear epileptic activity.

Two of these metrics, namely *Spectral Entropy* and *Cosine Similarity Entropy*, display this pattern also when the analysis was applied to the 5 sec window. The decrease in Conditional and Spectral entropies can be an indication that the system's behavior becomes more predictable and regular. The system passes to a less complex and more stable and repetitive state. On the other hand, the *Cosine Similarity Entropy* seems to give a contradictory result as it increases instead of decreasing. However, as the CoSiEn computation is based on the degree of self-correlation, an increase may indicate that the system in the ictal period displays a more repetitive behavior, which would be in accordance with the observation of the *Conditional* and *Spectral* entropies.

3.2 Results using the entire signal divided in four (4) time periods

We next repeated the analysis by separating the pre-Ictal period in two, based on the occurrence of the Spreading Depolarization (SD) event. This is an event that usually occurs only once and is considered a turning point in the transition to the epileptic state. Hence, we wanted to examine whether the various metrics could differentiate the period before and after this event, and to do this the comparison is done between 4 time periods: the Control period (as before), the pre-SD period (= the period from the switch to the 0 Mg condition to the onset of the SD), the post-SD period (from the SD event to the onset of SLEs), and finally the Ictal period (as before).

The results for the case of the whole signal analysis and the four (4) periods of interest, for 2 sec and 5 sec windows are summarized in Table 3 and Table 4.

Table 3: RANOVA results for the entire signal, 2 sec windows, 4 time periods

RANOVA Entire signal 2 sec windows, 4 periods	Control - PreSD	Control - PostSD	Control - Ictal	PreSD - PostSD	PreSD - Ictal	PostSD - Ictal
Metric						
Lyapunov Exponent			↘		↘	↘
Correlation Dimension					↘	↘
Approximate Entropy			↘		↘	↘
Sample Entropy			↘		↘	↘
Fuzzy Entropy						
Kolmogorov Entropy			↘		↘	↘
Permutation Entropy						
Conditional Entropy		↘	↘		~ ↘	↘
Distribution Entropy						
Spectral Entropy		~ ↘	↘			
Dispersion Entropy			↘		↘	↘
Increment Entropy						
Cosine Similarity Entropy		↗	↗			
Phase Entropy						
Bubble Entropy						
Renyi Entropy						↗
Entropy of Entropy			↘		~ ↘	↘
Average Shannon Entropy			↘		~ ↘	↘

Table 4: RANOVA results for the entire signal, 5 sec windows, 4 time periods

RANOVA, Entire signal 5 sec windows, 4 periods	Control - PreSD	Control - PostSD	Control - Ictal	PreSD - PostSD	PreSD - Ictal	PostSD - Ictal
Metric						
Lyapunov Exponent			↘		↘	↘
Correlation Dimension					~ ↘	↘
Approximate Entropy			↘			↘
Sample Entropy			↘			↘
Fuzzy Entropy						
Kolmogorov Entropy			↘		~ ↘	↘
Permutation Entropy						
Conditional Entropy			↘			↘
Distribution Entropy						
Spectral Entropy	~ ↘	~ ↘	~ ↘			
Dispersion Entropy			↘			↘
Increment Entropy						
Cosine Similarity Entropy		~ ↗	↗			
Phase Entropy						
Bubble Entropy						~ ↘
Renyi Entropy						↗
Entropy of Entropy			↘			↘
Average Shannon Entropy			↘			↘

The results show that there are no significant differences between the Control and the pre-SD periods, or pre-SD and the post-SD periods. On the other hand, the same metrics that showed a difference between the Control and the pre-Ictal period (in the case of the three periods case), now show a difference between the Control and post-SD period. We can infer that the system's behavior changes gradually after the 0 Mg condition

application and this change becomes more evident after the SD event. Once again there is a similarity between the 2 sec and 5 sec window cases indicating that the critical dynamics are evident in both time scales. This implies a consistency and stability in the systems behavior over time, especially regarding the two time scales, and suggests that the system's most important dynamics are well captured within the 2 sec time windows.

3.3 Results using the quiescent segments of the signal divided in three (3) time periods

We next decided to investigate whether transition network dynamics can be detected also during the quiescent periods. In this case the Phase Space Reconstruction analysis was performed selectively on the event-free segments of the recordings, ie the Down states of the control condition and the inter-event intervals of the pre-ictal and ictal conditions. The results of this analysis for 1 sec, 2 sec and 5 sec periods are shown in Table 5, Table 6 and Table 7. Boxplots of metrics of interest are shown in Figure 7 and Figure 8.

Table 5: RANOVA results for the quiescent periods, 1 sec windows, 3 time period

RANOVA Quiescent Periods 1 sec windows, 3 period	Control - Pre-ictal	Control - Ictal	Pre-ictal - Ictal
Metric			
Lyapunov Exponent			
Correlation Dimension			
Approximate Entropy			
Sample Entropy			
Fuzzy Entropy			
Kolmogorov Entropy			
Permutation Entropy			
Conditional Entropy	↘		
Distribution Entropy			
Spectral Entropy	↘		
Dispersion Entropy			
Increment Entropy			
Cosine Similarity Entropy	↗	↗ p=0.15	
Phase Entropy			
Bubble Entropy			
Renyi Entropy			
Entropy of Entropy			
Average Shannon Entropy			

We can see that three entropy metrics, namely Conditional, Spectral and the Cosine Similarity entropies, differentiate between the Control and the Pre-Ictal period in the same way we saw before, in the case of the entire signal analysis. In Figure 7 we can see the significant drop in the Conditional Entropy as we pass from the Control time period to the Pre-Ictal one. Figure 8 depicts the increase of Cosine Similarity Entropy in the Pre-Ictal period, compared to the Control one.

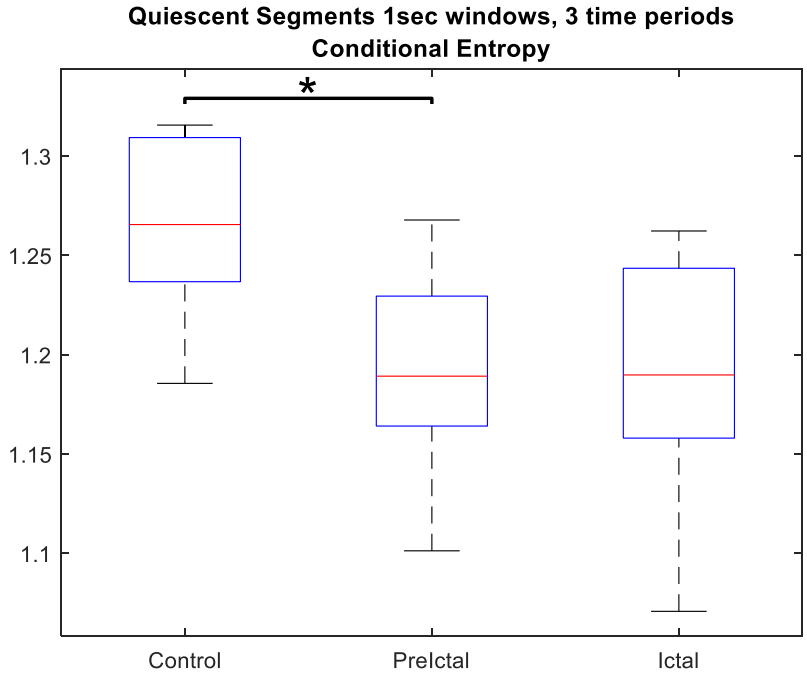

Figure 7: Conditional Entropy boxplot for the quiescent periods ,1 sec windows, 3 time periods (p-value = 0.029)

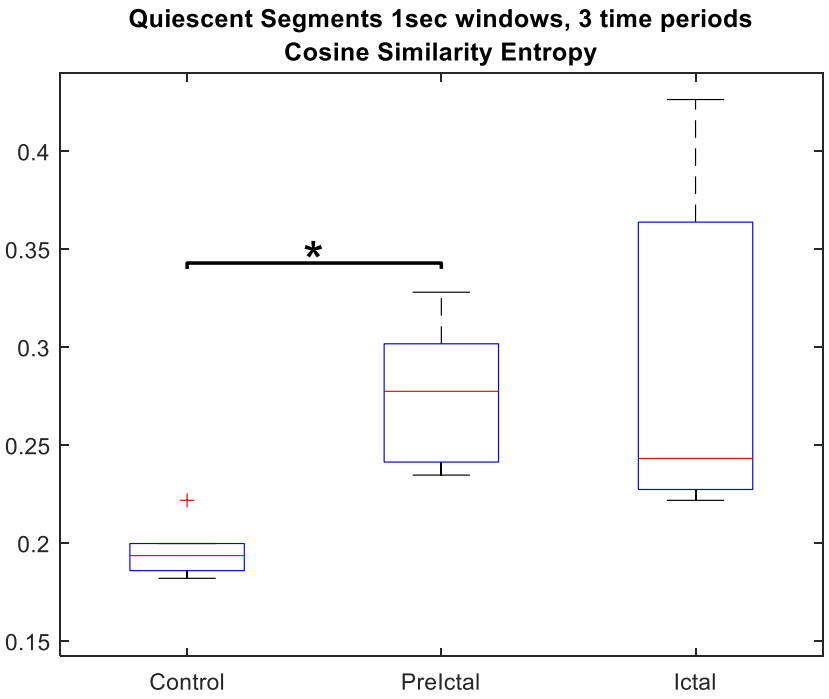

Figure 8: Cosine Similarity Entropy boxplot for the downstate signal 1sec windows, 3 time periods (p-value = 0.015)

In Table 6 the results for the quiescent periods analysis for the case of 2 sec windows and 3 time periods are presented. As we can see the results are identical to the case of the 1 sec windows.

Table 6: RANOVA results for the quiescent periods, 2 sec windows, 3 time periods

RANOVA Quiescent Periods 2 sec windows, 3 periods	Control - Pre-ictal	Control - Ictal	Pre-ictal - Ictal
Metric			
Lyapunov Exponent			
Correlation Dimension			
Approximate Entropy			
Sample Entropy			
Fuzzy Entropy			
Kolmogorov Entropy			
Permutation Entropy			
Conditional Entropy	↘		
Distribution Entropy			
Spectral Entropy	↘		
Dispersion Entropy			
Increment Entropy			
Cosine Similarity Entropy	↗		
Phase Entropy			
Bubble Entropy			
Renyi Entropy			
Entropy of Entropy			
Average Shannon Entropy			

Next, Table 7 summarizes the results for the quiescent periods analysis for the case of 5 sec windows and 3 time periods. For the case of the Conditional, Spectral and Cosine Similarity entropies, the results are the same as in the cases of the 1 sec and 2 sec windows.

Table 7: RANOVA results for the quiescent periods signal, 5 sec windows, 3 time periods

RANOVA Quiescent Periods 5sec windows, 3 periods	Control - Pre ictal	Control - Ictal	Pre-ictal - Ictal
Metric			
Lyapunov Exponent	↘		
Correlation Dimension			
Approximate Entropy			
Sample Entropy			
Fuzzy Entropy			
Kolmogorov Entropy			
Permutation Entropy			
Conditional Entropy	~↘ p=0.07		
Distribution Entropy			
Spectral Entropy	↘		
Dispersion Entropy			
Increment Entropy			
Cosine Similarity Entropy	↗		
Phase Entropy			
Bubble Entropy			
Renyi Entropy			
Entropy of Entropy			
Average Shannon Entropy			

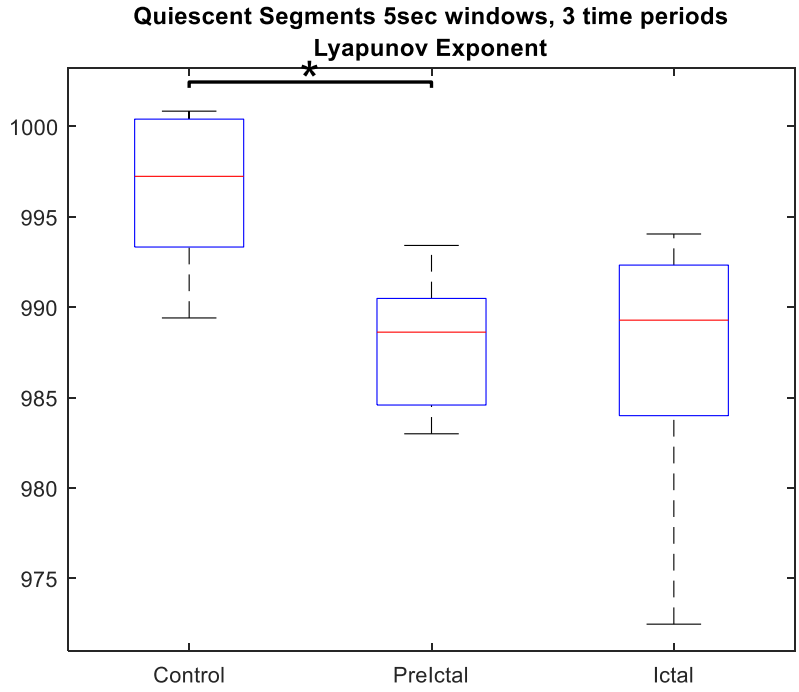

Figure 9: Lyapunov Exponent boxplot for the downstate signal,5sec windows, 3 time periods (p-value = 0.023)

Our results show that the same three entropy metrics, that appeared in the whole signal analysis, namely *Conditional*, *Spectral* and *Cosine Similarity* entropies, differentiate between the Control and the Pre-Ictal period for the 1sec and 2sec windows case, in the same way they did for the whole signal analysis. Furthermore, as we can see in Figure 9, the *Lyapunov exponent* is also significantly different between the Control period and the Pre-ictal period when the analysis was applied to the 5 sec window. The decrease of the Lyapunov exponent indicates that the system becomes more predictable and less sensitive to initial conditions.

3.4 Results using the quiescent segments of the signal divided in four (4) time periods

Results for the quiescent segments analysis with 1 sec windows and four periods the results are shown in Table 8. Boxplots for the Conditional Entropy and Cosine Similarity Entropy are shown in Figure 10 and Figure 11 respectively.

Table 8: RANOVA results for the quiescent segments signal, 1 sec windows, 4 time periods

RANOVA Quiescent Periods 1 sec windows, 4 periods	Control - PreSD	Control - PostSD	Control - Ictal	PreSD - PostSD	PreSD - Ictal	PostSD - Ictal
Metric						
Lyapunov Exponent						
Correlation Dimension						
Approximate Entropy						
Sample Entropy						
Fuzzy Entropy						
Kolmogorov Entropy						
Permutation Entropy						
Conditional Entropy		↘				
Distribution Entropy						
Spectral Entropy		~ ↘ p=0.075				
Dispersion Entropy						
Increment Entropy						
Cosine Similarity Entropy		↗				
Phase Entropy						
Bubble Entropy						
Renyi Entropy						
Entropy of Entropy						
Average Shannon Entropy						

We can see in Table 8 that when, by dividing the Pre-Ictal period to Pre-SD and Post-SD periods, Conditional and Cosine Similarity Entropies give us significant differences between the Control and the Post-SD period, similar to those we saw in the case of the three time periods between the Control and the Pre-Ictal periods. It seems that the differentiations we had between the Control and the Pre-Ictal periods are mostly due to dynamics' changes occurring during the Post-SD part of the Pre-Ictal period.

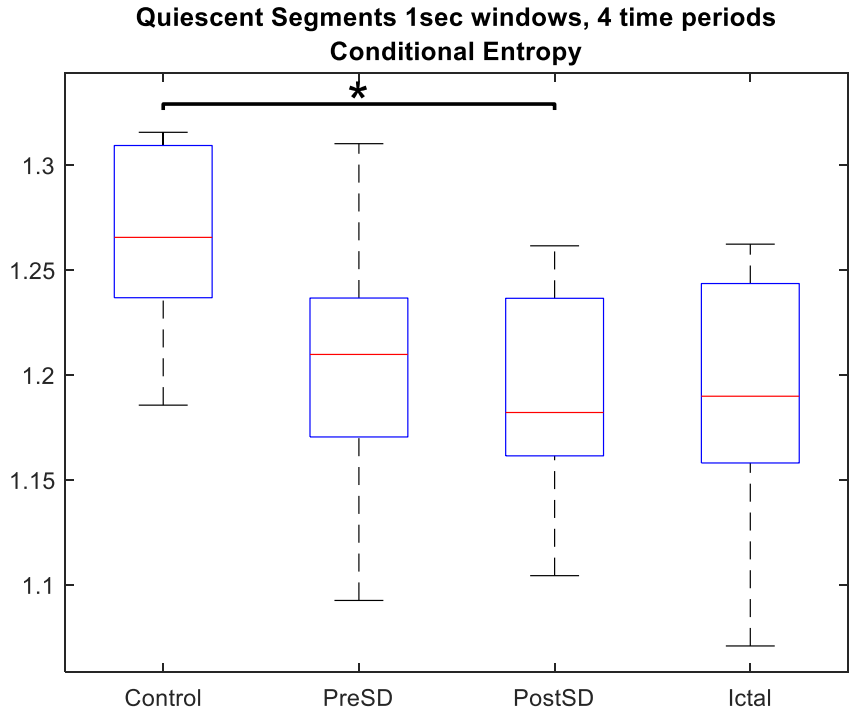

Figure 10: Conditional Entropy boxplot for the quiescent segments of the LFP signal (1 sec windows, 4 time periods, p-value = 0.049)

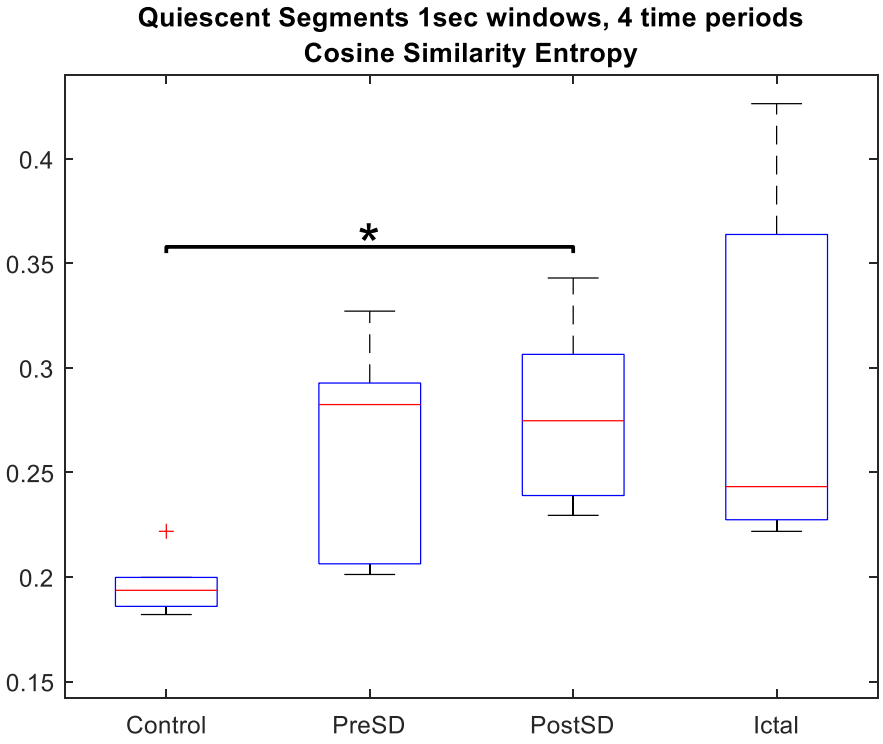

Figure 11: Cosine Similarity Entropy boxplot for the quiescent segments (1 sec windows, 4 time periods, p-value = 0.045)

Both Conditional and Cosine Similarity Entropies boxplots of Figures 10 and 11 depict the differentiation between the Control and the Post-SD periods. As in other cases we

may observe a tendency of “compensation” during the Ictal period.

The results for the quiescent segments analysis with 2 sec windows and four periods are shown in Table 9.

Table 9: RANOVA results for the quiescent segments, 2 sec windows, 4 time periods

RANOVA Quiescent Periods 2 sec window, 4 periods	Control - PreSD	Control - PostSD	Control - Ictal	PreSD - PostSD	PreSD - Ictal	PostSD - Ictal
Metric						
Lyapunov Exponent						
Correlation Dimension						
Approximate Entropy						
Sample Entropy						
Fuzzy Entropy						
Kolmogorov Entropy						
Permutation Entropy						
Conditional Entropy	~↘ p=0.063	↘				
Distribution Entropy						
Spectral Entropy		~↘ p=0.087				
Dispersion Entropy						
Increment Entropy						
Cosine Similarity Entropy		~↗ p=0.058				
Phase Entropy						
Bubble Entropy						
Renyi Entropy						
Entropy of Entropy						
Average Shannon Entropy						

The results for the 2 sec windows are almost identical to those of the 1 sec windows we saw before. It seems the dynamics of the system do not differentiate between these two time scales.

The results for the quiescent segments analysis with 5 sec windows and four periods the results are shown in Table 10.

Table 10: RANOVA results for the quiescent segments, 5 sec windows, 4 time periods

RANOVA Quiescent Periods 5 sec, 4 periods	Control - PreSD	Control - PostSD	Control - Ictal	PreSD - PostSD	PreSD - Ictal	PostSD - Ictal
Metric						
Lyapunov Exponent	↘	↘ p=0.068				
Correlation Dimension						
Approximate Entropy						
Sample Entropy						
Fuzzy Entropy						
Kolmogorov Entropy						
Permutation Entropy						
Conditional Entropy		↘ p=0.12				
Distribution Entropy						
Spectral Entropy		↘ p=0.094				
Dispersion Entropy						
Increment Entropy						
Cosine Similarity Entropy		↗ p=0.057				
Phase Entropy						
Bubble Entropy						
Renyi Entropy						
Entropy of Entropy						
Average Shannon Entropy						

For the case of the 5 sec windows, only the Lyapunov Exponent differentiates significantly between the Control and the Pre-SD periods. The corresponding boxplot is shown in Figure 12.

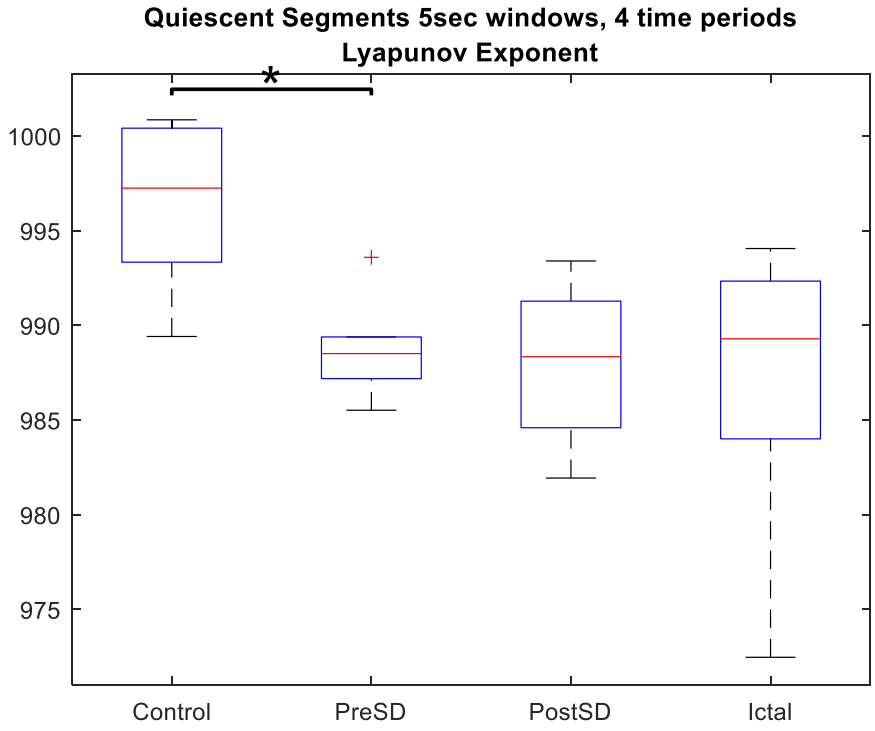

Figure 12: Lyapunov Exponent boxplot for the quiescent segments (5 sec windows, 4 time periods, p-value = 0.030)

This result is identical to the 5 sec and three time periods we saw before. The decrease of the Lyapunov exponent indicates that the system becomes more predictable and less sensitive to initial conditions.

Summarizing the results for the *quiescent segments* we can infer that after the application of the 0 Mg condition the system transits to a simpler, more predictable and repetitive state. It becomes more stable and less chaotic.

3.5 Results using the active segments of the signal divided in four (4) time periods

As a final step we applied the Phase Space Reconstruction analysis selectively only to the segments that include LFP events (either Up states in the control period, or interictal, SD or SLE events during the transition periods). Table 11 illustrates the results for 1 sec windows and four time periods. In Figure 12, the boxplot for Bubble Entropy is depicted.

Table 11: RANOVA results for the active segments of the signal, 1 sec windows, 4 time periods

RANOVA Active Segments, 1 sec windows, 4 periods	Control - PreSD	Control - PostSD	Control - Ictal	PreSD - PostSD	PreSD - Ictal	PostSD - Ictal
Metric						
Lyapunov Exponent						
Correlation Dimension						
Approximate Entropy						
Sample Entropy						
Fuzzy Entropy						
Kolmogorov Entropy						
Permutation Entropy						
Conditional Entropy						
Distribution Entropy						
Spectral Entropy						
Dispersion Entropy						
Increment Entropy						
Cosine Similarity Entropy						
Phase Entropy		↘				
Bubble Entropy	↘	↘		↘		
Renyi Entropy		↘				
Entropy of Entropy						
Average Shannon Entropy						

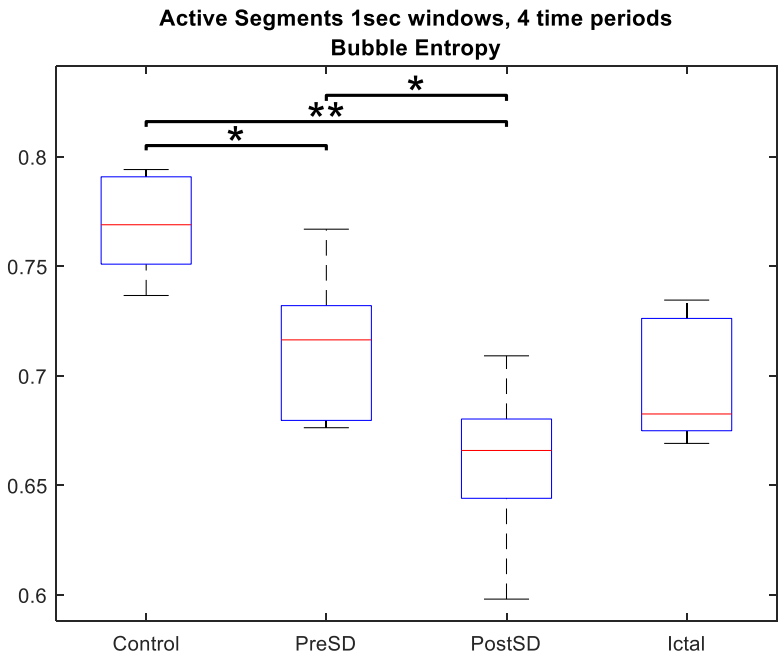

Figure 13: Bubble Entropy boxplot for the active segments of the signal (1 sec windows, 4 time periods, p-value Control-PreSD = 0.049, p-value Control-PostSD = 0,0052, p-value PreSD-PostSD = 0.048)

Bubble Entropy is of particular interest here as it is differentiated significantly between the

Control-PreSD, Control-PostSD and PreSD-PostSD periods.

Bubble Entropy is used to measure regularity and complexity in a time series. It was introduced by Manis et al. [25] as a very stable and descriptive metric, especially for analyzing physiology signals as heart rate ones. As shown in the boxplot of Figure 13 we have a gradual decrease in Bubble Entropy moving from the Control period to the Pre-SD and Post-SD periods. This decrease is firstly an indication of a dynamics' change between the time periods considered. Secondly, this dynamics change seems to include active segments that become more repetitive and predictable as time evolves. This graduate loss in complexity appears to be compensated by a short of "correction" in the epileptic period, an indication in favor of theories that consider the seizure like activity as correction response to previous loss of normal functionality. Phase Entropy and Renyi Entropy also point out a difference between the Control and the Post-SD events in the same sense.

3.6 Discussion

In all conditions examined (entire signal, quiescent segments, or active segments analysis), we observe that there are metrics that differentiate significantly between the Control and the Pre-Ictal periods. This was especially surprising in the case of the quiescent segment analysis, as such signals are usually considered trivial baseline signals of reduced interest.

These differences indicate important shifts in the dynamics of the system, even in the absence of observable activity. In all cases, these differences suggest that as the system leaves the default, spontaneous activity period and enters a state that will eventually lead to epilepsy, its behavior becomes gradually more regular, repetitive and predictable. We can infer that the system, on its way to epilepsy, undergoes a period, during which, it exhibits a less complex, less chaotic, and more regular and stable behavior. The identification of this gradual loss of complexity shown by the reduction in the values of the entropies discussed, could be used as a means of predicting epilepsy.

The Spreading Depolarization wave, is an event considered crucial for epilepsy, as its emergence signifies an almost certain transition to epilepsy. Our results, with the exception of those regarding the active periods (events) analysis, did not show significant importance of the SD event to the system's dynamics.

The observed reduction in entropy values when passing from the Control to the Pre-Ictal period can be attributed to a change from the complex dynamics of the normal brain behavior to that of a less complex, more regular and stable brain state. One could speculate that a disorganization of the brain dynamics that leads to loss of complexity, and increase of regularity, could eventually lead to the excess dynamics of epilepsy. Furthermore, our results include indications supporting theories that favor the epileptic state as an effort of correction on earlier alterations in brain's default dynamics [29].

4. CONCLUSION and FURTHER RESEARCH

The aim of this thesis is to study the transition from the default-spontaneous Up/Down states activity to the epileptiform activity using the reconstructed phase space methodology (PSR) and several non-linear metrics. As the brain activity evolves through time, starting from the spontaneous brain activity in the form of Up/Down states (Control period) and ending up in the stable epileptic state (Ictal or Seizure Like Activity period), we investigate for indications of changes in the complex dynamics of the underlying system.

Indeed, our results show that such changes do occur and are evident not only when examining the entire signal in its continuity but also when investigating the quiescent segments of the signal, and the active segments (i.e. events) of the signal. These changes are observed not only between the Pre-ictal and the Ictal periods as expected, but also between the Control and the Pre-ictal periods, a result that was not expected. Especially the quiescent segments case, is of particular interest, as such segments are considered in the relevant field literature of less importance regarding their contribution to the overall system dynamics.

Further work could aim at increasing the size of the data set. The data set used consists of six experiments on wild type mice. In several cases, metric comparisons between different time periods were found to be near statistical importance, that is with p-value larger than 0.05 but less than 0.10. A study on a larger dataset may provide more reliable conclusions. Moreover, one can use sliding windows instead of non-overlapping ones used here. Another issue of interest would be to compare the results of this study with results drawn from a data set consisting of mutant mice. It would be of interest to examine whether LFPs coming from these mice reveal similar patterns in the dynamics and behavior of the system as the wild-type ones. Another aspect of interest is that some of the experiments were not eventually led to epilepsy. One could investigate the factors that prevented the anticipated phenomenon development as also the corresponding emerged dynamics. Lastly, in our case the 0 Mg protocol is used to induce epilepsy. An investigation of whether, other epilepsy induction protocols such as the 4AP one, would produce results similar to ours or not, is of interest.

5. REFERENCES

[1] W. H. Organization. "Epilepsy." https://www.who.int/news-room/fact-sheets/detail/epilepsy (accessed.

[2] A. Destexhe, & Bedard, C. . "Local field potential." Scholarpedia. http://www.scholarpedia.org/article/Local_field_potential (accessed.

[3] G. Buzsaki, C. A. Anastassiou, and C. Koch, "The origin of extracellular fields and currents--EEG, ECoG, LFP and spikes," *Nat Rev Neurosci,* vol. 13, no. 6, pp. 407-20, May 18 2012, doi: 10.1038/nrn3241.

[4] P. Rigas, D. A. Adamos, C. Sigalas, P. Tsakanikas, N. A. Laskaris, and I. Skaliora, "Spontaneous Up states in vitro: a single-metric index of the functional maturation and regional differentiation of the cerebral cortex," *Front Neural Circuits,* vol. 9, p. 59, 2015, doi: 10.3389/fncir.2015.00059.

[5] M. Zijlmans, J. Jacobs, R. Zelmann, F. Dubeau, and J. Gotman, "High frequency oscillations and seizure frequency in patients with focal epilepsy," *Epilepsy Res,* vol. 85, no. 2-3, pp. 287-92, Aug 2009, doi: 10.1016/j.eplepsyres.2009.03.026.

[6] S. A. Weiss *et al.*, "Ictal onset patterns of local field potentials, high frequency oscillations, and unit activity in human mesial temporal lobe epilepsy," *Epilepsia,* vol. 57, no. 1, pp. 111-21, Jan 2016, doi: 10.1111/epi.13251.

[7] S. H. Strogatz, *Nonlinear dynamics and chaos : with applications to physics, biology, chemistry, and engineering*, Second edition. ed. Boulder, CO: Westview Press, a member of the Perseus Books Group, 2015, pp. xiii, 513 pages.

[8] A. Dawid, "PSR-based research of feature extraction from one-second EEG signals: a neural network study," *SN Applied Sciences,* vol. 1, no. 12, p. 1536, 2019/11/04 2019, doi: 10.1007/s42452-019-1579-9.

[9] F. Takens, "Detecting strange attractors in turbulence," in *Dynamical Systems and Turbulence, Warwick 1980*, Berlin, Heidelberg, D. Rand and L.-S. Young, Eds., 1981// 1981: Springer Berlin Heidelberg, pp. 366-381.

[10] N. H. Packard, J. P. Crutchfield, J. D. Farmer, and R. S. Shaw, "Geometry from a Time Series," *Physical Review Letters,* vol. 45, no. 9, pp. 712-716, 09/01/ 1980, doi: 10.1103/PhysRevLett.45.712.

[11] D. P. Feldman, *Chaos and dynamical systems.* . Princeton University Press. , 2019.

[12] E. Bradley and H. Kantz, "Nonlinear time-series analysis revisited," *Chaos: An Interdisciplinary Journal of Nonlinear Science,* vol. 25, no. 9, p. 097610, 2015, doi: 10.1063/1.4917289.

[13] S.-H. Lee, J. S. Lim, J.-K. Kim, J. Yang, and Y. Lee, "Classification of normal and epileptic seizure EEG signals using wavelet transform, phase-space reconstruction, and Euclidean distance," *Computer Methods and Programs in Biomedicine,* vol. 116, no. 1, pp. 10-25, 2014/08/01/ 2014, doi: https://doi.org/10.1016/j.cmpb.2014.04.012.

[14] R. Sharma and R. B. Pachori, "Classification of epileptic seizures in EEG signals based on phase space representation of intrinsic mode functions," *Expert Systems with Applications,* vol. 42, no. 3, pp. 1106-1117, 2015/02/15/ 2015, doi: https://doi.org/10.1016/j.eswa.2014.08.030.

[15] N. Vasilopoulos *et al.*, "The role of selective SATB1 deletion in somatostatin expressing interneurons on endogenous network activity and the transition to epilepsy," *Journal of Neuroscience Research,* vol. 101, no. 4, pp. 424-447, 2023/04/01 2023, doi: https://doi.org/10.1002/jnr.25156.

[16] N. Hajos *et al.*, "Maintaining network activity in submerged hippocampal slices: importance of oxygen supply," *Eur J Neurosci,* vol. 29, no. 2, pp. 319-27, Jan 2009,

doi: 10.1111/j.1460-9568.2008.06577.x.

[17] R. J. Harris, T. Wieloch, L. Symon, and B. K. Siesjö, "Cerebral Extracellular Calcium Activity in Severe Hypoglycemia: Relation to Extracellular Potassium and Energy State," *Journal of Cerebral Blood Flow & Metabolism,* vol. 4, no. 2, pp. 187-193, 1984/06/01 1984, doi: 10.1038/jcbfm.1984.27.

[18] H. C. Jones and R. F. Keep, "Brain fluid calcium concentration and response to acute hypercalcaemia during development in the rat," *J Physiol,* vol. 402, pp. 579-93, Aug 1988, doi: 10.1113/jphysiol.1988.sp017223.

[19] C. Sigalas, P. Rigas, P. Tsakanikas, and I. Skaliora, "High-Affinity Nicotinic Receptors Modulate Spontaneous Cortical Up States In Vitro," *J Neurosci,* vol. 35, no. 32, pp. 11196-208, Aug 12 2015, doi: 10.1523/JNEUROSCI.5222-14.2015.

[20] M. W. Flood and B. Grimm, "EntropyHub: An open-source toolkit for entropic time series analysis," *PLOS ONE,* vol. 16, no. 11, p. e0259448, 2021, doi: 10.1371/journal.pone.0259448.

[21] A. Porta *et al.*, "Measuring regularity by means of a corrected conditional entropy in sympathetic outflow," *Biological Cybernetics,* vol. 78, no. 1, pp. 71-78, 1998/01/01 1998, doi: 10.1007/s004220050414.

[22] T. Chanwimalueang and D. P. Mandic, "Cosine Similarity Entropy: Self-Correlation-Based Complexity Analysis of Dynamical Systems," *Entropy*, vol. 19, no. 12*,* doi: 10.3390/e19120652.

[23] H. Helakari *et al.*, "Spectral entropy indicates electrophysiological and hemodynamic changes in drug-resistant epilepsy – A multimodal MREG study," *NeuroImage: Clinical,* vol. 22, p. 101763, 2019/01/01/ 2019, doi: https://doi.org/10.1016/j.nicl.2019.101763.

[24] T. Inouye *et al.*, "Quantification of EEG irregularity by use of the entropy of the power spectrum," *Electroencephalography and Clinical Neurophysiology,* vol. 79, no. 3, pp. 204-210, 1991/09/01/ 1991, doi: https://doi.org/10.1016/0013-4694(91)90138-T.

[25] G. Manis, M. Aktaruzzaman, and R. Sassi, "Bubble Entropy: An Entropy Almost Free of Parameters," *IEEE Transactions on Biomedical Engineering,* vol. 64, no. 11, pp. 2711-2718, 2017, doi: 10.1109/TBME.2017.2664105.

[26] Y. Yin, K. Sun, and S. He, "Multiscale permutation Renyi entropy and its application for EEG signals," *PLoS One,* vol. 13, no. 9, p. e0202558, 2018, doi: 10.1371/journal.pone.0202558.

[27] M. A. Rahman, F. Khanam, M. Ahmad, and M. S. Uddin, "Multiclass EEG signal classification utilizing Renyi min-entropy-based feature selection from wavelet packet transformation," *Brain Inform,* vol. 7, no. 1, p. 7, Jun 16 2020, doi: 10.1186/s40708-020-00108-y.

[28] L. D. Iasemidis *et al.*, "Adaptive epileptic seizure prediction system," *IEEE Transactions on Biomedical Engineering,* vol. 50, no. 5, pp. 616-627, 2003, doi: 10.1109/TBME.2003.810689.

[29] J. Sackellares, L. Iasemidis, R. Gilmore, and S. Roper, "Epilepsy - When Chaos Fails," 02/03 2000, doi: 10.1142/9789812793782_0010.

6. APPENDIX

The Matlab scripts used, as well as the data from one of the experiments can be found here: https://zenodo.org/records/10719854

Script1 loads the mat files and calculates the metrics for each time window for the entire signal of each of the five 20min long recordings. It stores the results in an excel file. The results in these excel files, for the case of the last four 20min recordings, are manually rearranged in the Pre-Ictal (or PreSD, PostSD) and Ictal periods, depending on when the first seizure like event emerges (and when the SD event occurs for the case of the four period analysis). Then the average values (for each metric) are computed for each time period of interest, for each experiment. The results are stored in a new excel file which is the input of Script2.

Script2 takes as input an excel file containing the mean values of each metric for each of the periods of interest (Control, Pre-Ictal, Ictal) for each the six experiments, as stated above, and performs RANOVA tests between these periods.

For the case of the quiescent or the active parts analysis, specific, appropriate in each case parts of the signal, are chosen instead of the entire signal. The rest of the analysis proceeds as before.

For further information and access to the data used please contact:

Skaliora Lab, Brain Electrophysiology, Center of Basic Research, Biomedical Foundation of the Academy of Athens (BRFAA), iskaliora@bioacademy.gr